Quaternary International 311 (2013) 97–107

Contents lists available at SciVerse ScienceDirect

Quaternary International

journal homepage: www.elsevier.com/locate/quaint

Changes in precipitation extremes in alpine areas of the Chinese Tianshan Mountains, central Asia, 1961–2011

Shengjie Wang, Mingjun Zhang*, Meiping Sun, Baolong Wang, Xiaofei Li

College of Geography and Environmental Science, Northwest Normal University, Lanzhou, Gansu 730030, China

ARTICLE INFO

Article history:
Available online 27 July 2013

ABSTRACT

Based on the gridded and observed daily precipitation datasets from 1961 to 2011, changes in daily precipitation extremes in alpine areas of the Chinese Tianshan Mountains are discussed. Four indices that represent extreme precipitation events are selected and calculated. Maximum 5-day precipitation, simple daily intensity index and very wet day precipitation have increased significantly by 1.18 mm, 0.09 mm/d, and 6.75 mm per decade, respectively, while consecutive dry days have decreased at a rate of 5.83 days per decade during the study period. Changes in probability distribution functions of precipitation indices before and after the detected abrupt year also indicate a wetting trend. Generally, the linear trends of precipitation indices are spatially coherent. Approximately 79.0%, 83.8%, and 98.1% of the grid boxes show increasing trends for maximum 5-day precipitation, simple daily intensity index and very wet day precipitation, respectively, and the proportion of decreasing trends for consecutive dry days is 95.2%. Trends in most precipitation indices (except consecutive dry days) are highly correlated with total precipitation trends ($p < 0.0001$). Significant correlations between precipitation indices and Northern Hemisphere Annular Mode Index (also referred as Arctic Oscillation Index) in wintertime indicate that precipitation extremes in the study area are related to the Arctic Oscillation.

© 2013 Elsevier Ltd and INQUA. All rights reserved.

1. Introduction

Due to the low precipitation and high evaporation, water scarcity is one of the core issues in arid central Asia (Vörösmarty et al., 2000; Hoekstra et al., 2012). In the past decades, this region has experienced a climatic and environmental change (Lioubimtseva and Henebry, 2009), which has been widely recognized from precipitation (Small et al., 1999; Lioubimtseva et al., 2005; Schiemann et al., 2008), runoff (Kezer and Matsuyama, 2006; Li et al., 2010), glacier (Aizen et al., 2006; Bolch, 2007; Narama et al., 2010; Wang et al., 2011), and permafrost (Marchenko et al., 2007; Zhao et al., 2010a). Among these hydro-climatic variables, atmospheric precipitation plays a vital role in water budget (Getirana et al., 2011). Warming is expected to accelerate the hydrological cycle and precipitation will increase on average (Oki and Kanae, 2006).

In arid central Asia, most precipitation takes place in high-altitude alpine regions. For example, in Xinjiang, Northwest China, the proportion of precipitation in mountainous areas is up to 84% (Zhang and Zhang, 2006). The Tianshan Mountains are located in arid central Asia, and have relatively abundant rainfall, larger than the regional mean (Schiemann et al., 2008). During the period 1940–1991, annual precipitation has increased by 1.2 mm per year over the Tianshan Mountains (Aizen et al., 1997). The climate in Northwest China changed dramatically from a warm-dry mode to a warm-wet mode around 1987, and the Chinese Tianshan Mountains experienced the most dramatic changes during this transition (Shi et al., 2007). Later studies have further affirmed the general wetting trend (e.g., Zhang et al., 2012b; Wang et al., 2011; Wang H. et al., 2013a). However, existing reports mainly cover the low-lying plains, and the high-altitude areas are relatively unknown in terms of recent climate changes simply due to lack of meteorological observations. Therefore, high-altitude areas in the Chinese Tianshan Mountains await in-depth investigations into climate change.

In order to investigate the recent changes in frequency, intensity and duration of precipitation extremes in alpine areas of the Chinese Tianshan Mountains, gridded and observed daily precipitation during the period 1961–2011 were collected from the China Meteorological Administration (CMA), and several widely-applied indices are calculated. Changes in the selected precipitation indices as well as the relationship between precipitation extremes and atmospheric circulation are analyzed in this paper.

* Corresponding author.
E-mail address: mjzhang2004@163.com (M. Zhang).

1040-6182/$ – see front matter © 2013 Elsevier Ltd and INQUA. All rights reserved.
http://dx.doi.org/10.1016/j.quaint.2013.07.008

2. Data and methods

2.1. Meteorological data and quality control

2.1.1. Gridded data

In this study, the gridded daily precipitation dataset (China's Ground Precipitation 0.5° × 0.5° Grid Dataset V2.0) is provided by the National Meteorological Information Center (NMIC) of the China Meteorological Administration (CMA). According to the contour lines of 1500 m a.s.l. (above sea level), 105 grid boxes are selected to describe the alpine areas of the Chinese Tianshan Mountains (Fig. 1). The daily observations from 1961 to the present at 2472 gauges over the Chinese mainland are assimilated into this dataset. The monthly RMSE (root-mean-square error) generally ranges from 0.2 mm to 0.8 mm, and the mean level is 0.49 mm. The seasonal MBE (mean bias error) are −0.1, −0.3, −0.8 and −0.3 mm per month in winter (JJA), spring (MAM), summer (JJA) and autumn (SON), respectively. More details about the calculation process and error analysis are described by NMIC (2012).

2.1.2. Observed data

In order to validate the gridded data, the observed daily precipitation was also acquired from NMIC. In the observation network of CMA, most meteorological stations over the Chinese Tianshan Mountains are located at the low-lying plains. Only 12 stations above 1500 m have maintained daily observations since 1961. In this study, 4 of these are rejected because of data accessibility and continuity, so 8 observational stations are selected (Fig. 1 and Table 1). The altitude of these selected stations ranges from 1677 m (Barkol) to 3504 m (Torugart). Monthly distributions of precipitation for each station are shown in Fig. 2.

Table 1
List of observation stations with WMO (World Meteorological Organization) number, latitude, longitude, altitude, annual temperature and precipitation (standard climatological normal, 1971–2010).

WMO number	Station name	Latitude (°N)	Longitude (°E)	Altitude (m)	Temperature (°C)	Precipitation (mm)
51705	Wuqia	39.72	75.25	2176	7.3	172.8
51701	Torugart	40.52	75.40	3504	−3.3	236.9
51711	Akqi	40.93	78.45	1985	6.5	209.9
51437	Zhaosu	43.15	81.13	1851	3.3	492.2
51542	Bayanbulak	43.03	84.15	2458	−4.5	268.8
51467	Baluntai	42.73	86.30	1739	6.4	216.4
52101	Barkol	43.60	93.05	1677	1.8	220.3
52118	Yiwu	43.27	94.70	1729	3.9	103.4

Data quality control is a prerequisite in climate change research. For the observed daily precipitation, a series of strict quality controls (including checks for high-low extreme values and time consistency) are employed, and errors are corrected by NMIC (Li and Xiong, 2004; Wang, 2004). After that, a simple quality control is operated using RClimDex V1 software (Zhang and Yang, 2004). Homogeneity assessment of raw data is processed with RHtest V3 software (Wang, 2008). Both RClimDex V1 and RHtest V3 are obtainable from http://etccdi.pacificclimate.org. With the help of the latter program, possible change points in a precipitation series can be detected and adjusted. As for the stations in this study, there is only one station (Zhaosu) with potential steps in 1967 and 1997. However, around the corresponding years, no valid explanation can be found in the metadata including documented station relocation and instrument updating. Subsequent adjustments were not applied.

2.2. Extreme precipitation indices calculation

The ETCCDI (Expert Team on Climate Change Detection and Indices) is a joint project of the World Meteorological Organization's Commission for Climatology (CCl), the World Climate Research Programme's Climate Variability and Predictability (CLIVAR), and the Joint Technical Commission for Oceanography and Marine Meteorology (JCOMM). Four precipitation indices are selected from the core indices list recommended by the Joint CCl-CLIVAR-JCOMM ETCCDI (http://etccdi.pacificclimate.org) (Table 2). These selected indices are widely used to assess the changes in daily precipitation extremes (Klein Tank et al., 2006; Caesar et al., 2011; Vincent et al., 2011; You et al., 2011; Wang S. et al., 2013), and can be calculated using RClimDex V1 software. Some indices in the full list which are not relevant to the high-altitude areas are excluded in this study. For instance, the consecutive wet days (CWD, i.e. maximum number of consecutive days with precipitation > 1 mm) show low values and slight variation ranges, so the index is not discussed here.

Table 2
Definitions of precipitation indices used in this study.

Index (Unit)	Descriptive name	Definition
RX5day (mm)	Maximum 5-day precipitation	Annual maximum consecutive 5-day precipitation
SDII (mm/d)	Simple daily intensity index	Average daily precipitation when precipitation ≥ 1 mm
CDD (d)	Consecutive dry days	Maximum number of consecutive days with precipitation < 1 mm
R95p (mm)	Very wet day precipitation	Annual total precipitation when daily precipitation > 95th percentile of days with precipitation ≥ 1 mm from 1961 to 2011

2.3. Northern Hemisphere Annular Mode Index

Over the Chinese Tianshan Mountains, the regime is mainly controlled by the Westerlies in the Northern Hemisphere all year-round. Arctic Oscillation (AO) as well as North Atlantic Oscillation (NAO) reflect the strength of the Westerlies in middle latitude of the Northern Hemisphere (Thompson and Wallace, 2000; Ogi et al., 2003). In the positive phase of AO/NAO with enhancements of Azores High and Icelandic Low in the North Atlantic, northern Eurasia may receive more rainfall than the mean. Previous research on precipitation in China also confirms this regime (Gong and Ho, 2003; Ju et al., 2005; Gu et al., 2009).

The monthly Northern Hemisphere Annular Mode Index (NAMI, also referred as Arctic Oscillation Index, AOI) is defined as the difference in the normalized monthly zonal-mean sea level pressure (SLP) between 35°N and 65°N (Li and Wang, 2003). Data from 1961 to 2011 used in this study is acquired from Li's homepage of the State Key Laboratory of Numerical Modeling for Atmospheric Sciences and Geophysical Fluid Dynamics (LASG) at http://ljp.lasg.ac.cn. Sea level pressure used in the calculation is

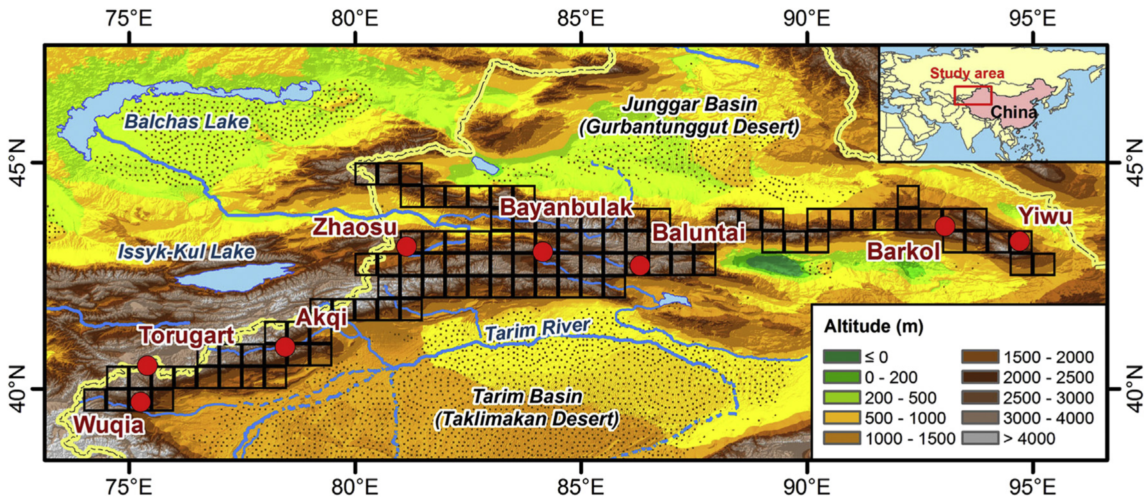

Fig. 1. Locations of selected grid boxes (squares) and observation stations (points) in alpine areas of the Chinese Tianshan Mountains. Dashed lines denote China's national boundaries. Locations of deserts are modified from Wang et al. (2005).

from three data sources, including Hadley Centre (1850 to present), NCEP1 (1948 to present) and NCAR (1899 to present), respectively.

2.4. Trend estimation and test method

The nonparametric Sen's method (Sen, 1968) is employed to calculate the trends for precipitation indices. A trend is considered to be statistically significant if it is significant at the 0.05 level (if without additional description) using a Mann–Kendall test (Kendall, 1955). These nonparametric methods do not assume that the data series is normally distributed, which is widely used in precipitation-related research (Vincent et al., 2011). A sequential Mann–Kendall test (Sneyers, 1990) is also applied to examine the abrupt year for annual total precipitation. For correlation coefficient, Pearson's correlation and two-tailed *t*-test are used. Regional series of precipitation indices over the Chinese Tianshan Mountains is calculated as an arithmetic mean of values for each station or grid box.

3. Results

3.1. Changes in precipitation extremes

As shown in Fig. 3a and b, annual total precipitations derived from gridded and observed data show increasing trends, respectively. The trend magnitudes are 14.8 and 12.1 mm per decade, respectively, which are statistically significant at the 0.001 level. Their patterns are generally coherent, which can be detected from the peaks in the late 1990s, mid 1980s and other characteristic points. According to a sequential Mann–Kendall test (Fig. 3c and d), a significant step change is found in 1992, similar to previous studies (Li and Jiang, 2007). These results also indicate that the alpine precipitation can be described accurately using this gridded dataset. However, the gridded precipitation is much higher than the observed precipitation, which is mainly caused by the uneven distribution of observation stations. For the annual total precipitation derived from the gridded dataset, 98.1% of grid boxes show positive trends and 58.1% are statistically significant at the 0.05 level.

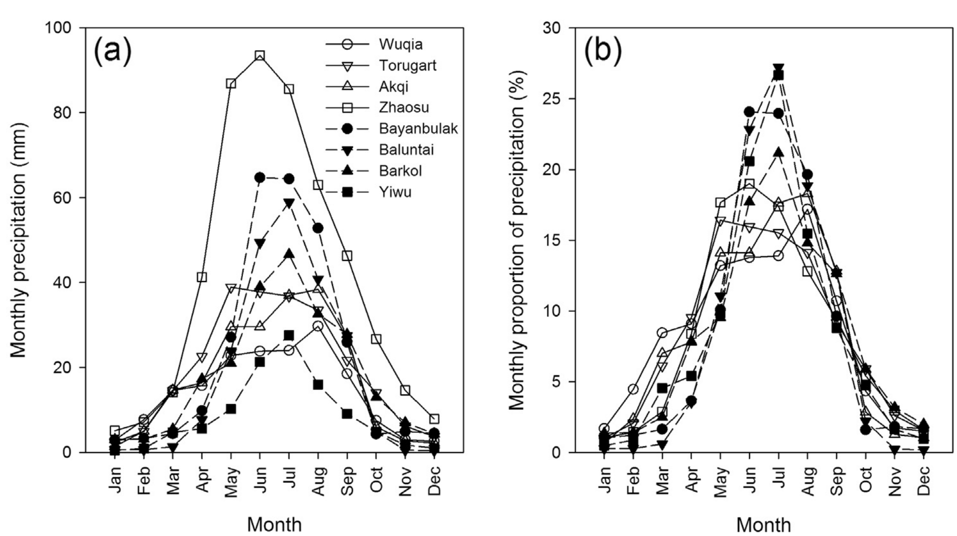

Fig. 2. Monthly distributions of precipitation for observation stations in alpine areas of the Chinese Tianshan Mountains (standard climatological normal, 1971–2010).

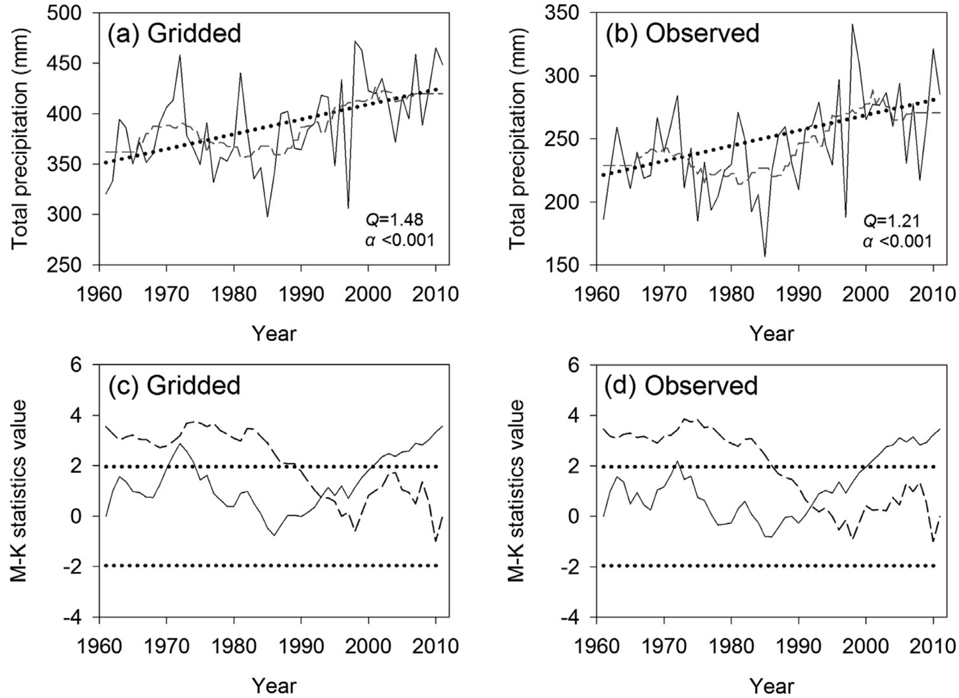

Fig. 3. Annual series (a and b) and sequential Mann–Kendall analysis result (c and d) of gridded and observed total precipitation. In a and b, dotted lines denote Sen's estimates, and grey dashed curves denote 10-year running averages. *Q* is Sen's slope in mm per year, and *α* is significant level of Mann–Kendall test. In c and d, solid and dashed lines denote forward and backward series, respectively, and horizontal dotted lines denote the 0.05 confidence level.

With such a wetting trend, the extreme precipitation events also show contemporaneous changes. According to the definitions, the four precipitation indices can be divided into wet indices (i.e. maximum 5-day precipitation, simple daily intensity index, and very wet day precipitation) and dry indices (i.e. consecutive dry days). Based on the gridded data, three wet indices all have positive trends during the study period (Fig. 4a, b and d). Maximum 5-day precipitation (RX5day) shows an

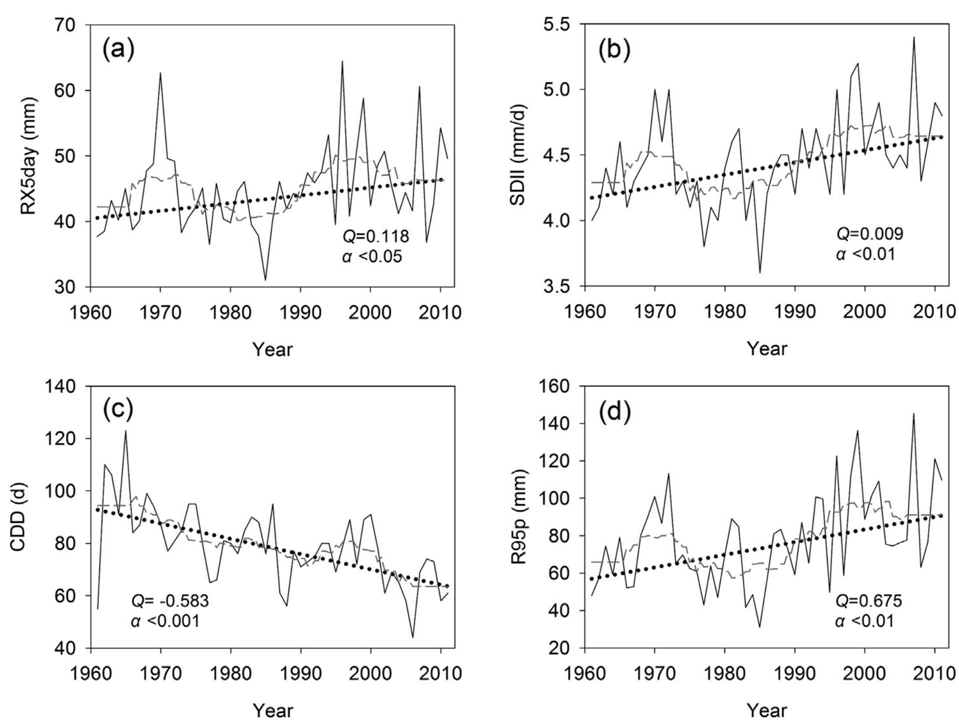

Fig. 4. Changes in maximum 5-day precipitation (a), simple daily intensity index (b), consecutive dry days (c) and very wet day precipitation (d) derived from gridded data. Dotted lines denote Sen's estimates, and grey dashed curves denote 10-year moving averages. *Q* is Sen's slope in mm, mm/d, d and mm per year respectively, and *α* is significant level of Mann–Kendall test.

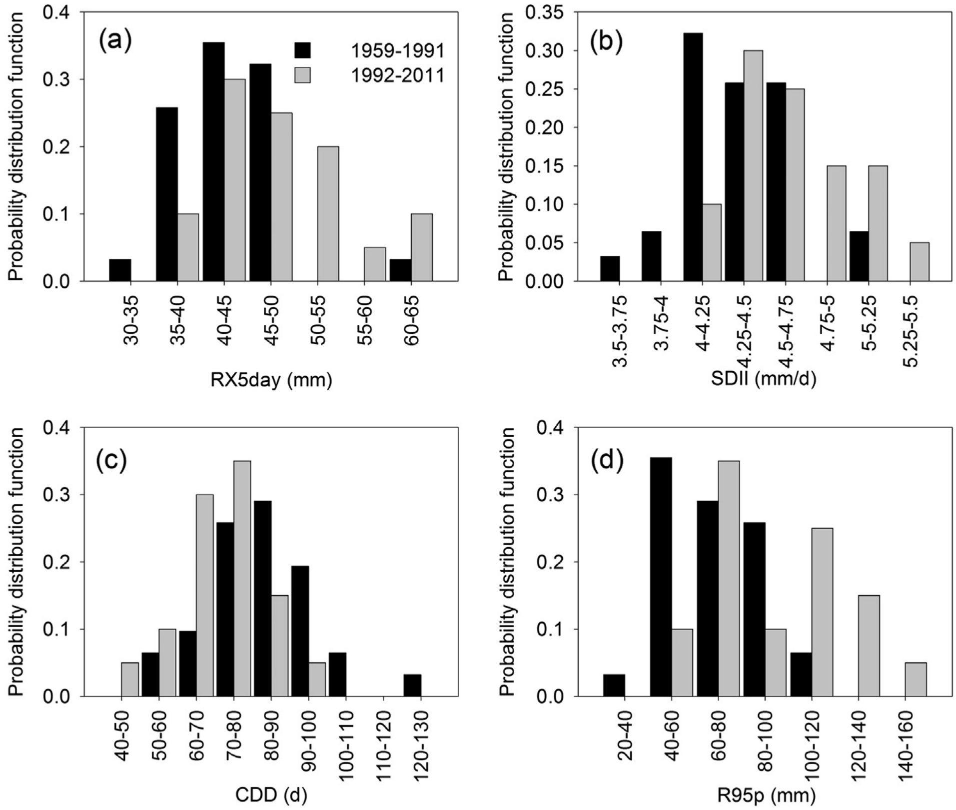

Fig. 5. Probability distribution functions of maximum 5-day precipitation (a), simple daily intensity index (b), consecutive dry days (c) and very wet day precipitation (d) derived from gridded data.

increasing trend of 1.18 mm per decade, which is statistically significant at the 0.05 level. Simple daily intensity index (SDII) has significantly increased at a rate of 0.09 mm/d per decade ($p < 0.01$). The regional trend of very wet day precipitation (R95p) reaches up to 6.75 mm per decade ($p < 0.01$). In addition, wet indices generally show high values in the period from the late 1960s to the early 1970s, as well as the period from the 1990s to the early 2000s. Oppositely, the regional series of consecutive dry days (CDD) shows a statistically significant decrease at a rate of 5.83 days per decade, and the wave pattern is different from the wet indices (Fig. 4c).

According to the abrupt year (1992) detected in the above section, the probability distribution functions (PDFs) of each precipitation index are calculated for two periods respectively, that is, 1961–1991 and 1992–2011 (Fig. 5). Significant shifts can be found from the PDFs in different periods. For example, high probability values of maximum 5-day precipitation (RX5day) have changed from 30–40 mm to 35–45 mm between the two periods, and probability of 50–65 mm has increased significantly (Fig. 5a). The maximum interval of simple daily intensity index (SDII) has shifted from 4 to 4.25 mm/d to 4.25–4.5 mm/d, and the probability of low-SDII (lower than 4 mm/d) even has decreased to zero (Fig. 5b). Shifts of probability distribution can also be determined for other indices (Fig. 5c and d).

As is demonstrated in Fig. 6 and Table 3, most grid boxes for each precipitation index exhibit the same positive or negative trends, showing spatial coherence. For maximum 5-day precipitation (RX5day), about 79.0% of grid boxes show increasing trends at a rate of 1.60 mm per decade, and 20.0% are statistically significant at the 0.05 level. The largest trend magnitudes generally occur at the western mountain ranges centered near the Akqi station. For simple daily intensity index (SDII), the percentage of grid boxes with increasing trends is up to 83.8%, and 38.1% are statistically significant at the 0.05 level. Distinct from other indices, 14.3% of grid boxes for SDII show stable trends during the study period. For consecutive dry days (CDD), 95.2% of grid boxes show decreasing tendencies at −5.83 days per decade, and statistically significant trends occur in more than half of grid boxes (57.1%). Low-value regions for wet indices are generally corresponding to the high-value regions for CDD. For very wet day precipitation (R95p), 98.1% of grid boxes have increasing trends, and 30.5% are statistically significant at the 0.05 level. The observed trends are commonly consistent with the gridded ones.

Table 3
Proportions and trend magnitudes of grid boxes with negative and positive trends for each precipitation index derived form gridded data.

	Indices	Unit	Increasing trend		Stable	Decreasing trend	
			Sig. & Insig.	Sig.		Sig. & Insig.	Sig.
Proportion	RX5day	%	79.0	20.0	0.0	21.0	0.0
	SDII	%	83.8	38.1	14.3	1.9	0.0
	CDD	%	4.8	0.0	0.0	95.2	57.1
	R95p	%	98.1	30.5	0.0	1.9	0.0
Trend	RX5day	mm/decade	1.60	3.09	–	−0.73	–
	SDII	mm/d/decade	0.12	0.18	0	−0.06	–
	CDD	d/decade	0.88	–	–	−5.83	−6.96
	R95p	mm/decade	6.51	9.80	–	−1.24	–

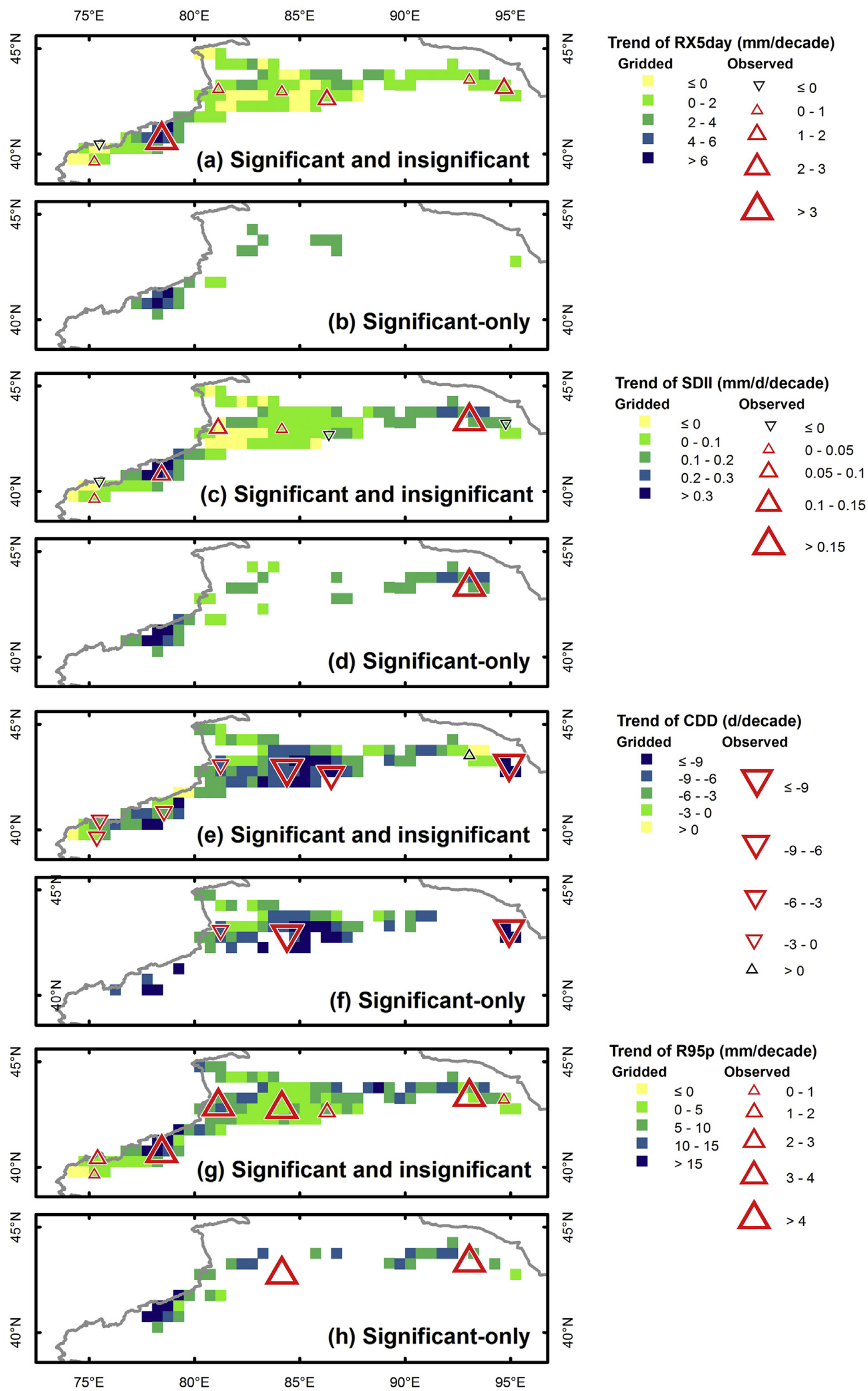

Fig. 6. Trends in annual series for maximum 5-day precipitation (a and b), simple daily intensity index (c and d), consecutive dry days (e and f) and very wet day precipitation (g and h).

3.2. Relationship between precipitation extremes and total precipitation

Correlations between trend magnitudes of precipitation extremes and total precipitation are presented in Fig. 7. Total precipitations correlate positively with maximum 5-day precipitation (RX5day), simple daily intensity index (SDII) and very wet day precipitation (R95p), and consecutive dry days (CDD) show a negative correlation with total precipitation. Correlation coefficients between precipitation extremes and totals are 0.94,

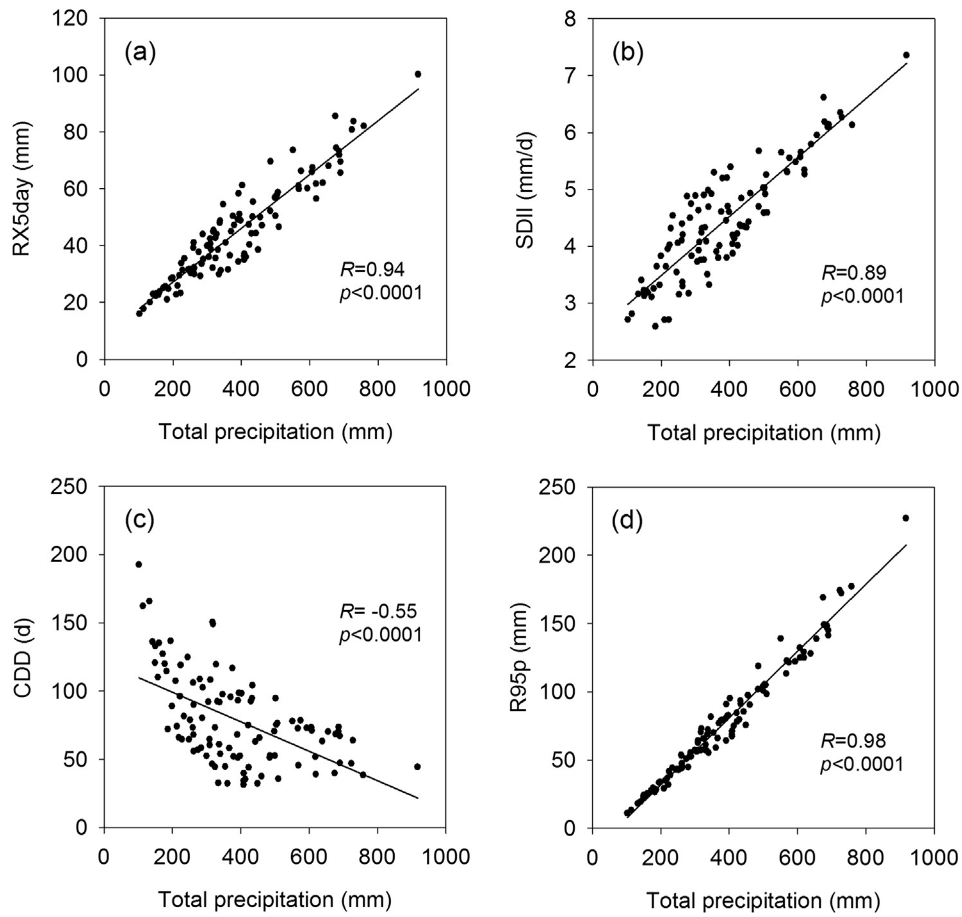

Fig. 7. Correlation between annual magnitudes between precipitation indices and total precipitation ($N = 105$). R is correlation coefficient, and p is significant level of t-test.

0.89, −0.55 and 0.98 for RX5day, SDII, CDD and R95p, respectively ($p < 0.0001$). Trends in precipitation extremes are highly correlated with total precipitation trends (Fig. 8). Correlations between trends in total precipitation and three wet indices are 0.80, 0.74 and 0.66 for RX5day, SDII and R95p, respectively ($p < 0.0001$). Different from the wet indices, trends in consecutive dry days (CDD) show an insignificant correlation with total precipitation ($R = 0.16$, $p = 0.09$).

The ratio between very wet day precipitation (R95p) and annual total precipitation shows an increasing trend at a rate of approximate 1% per decade ($p < 0.05$) (Fig. 9). The contribution of precipitation on very wet days to total amounts ranges from 9.4% to 32.8%. Although the similar increasing trend has been reported for other regions in China (You et al., 2008; Li et al., 2012), the trend magnitudes in alpine areas of the Chinese Tianshan Mountains are larger than those in previous studies.

3.3. Relationship between precipitation extremes and atmospheric circulation

Table 4 demonstrates the correlation coefficients between precipitation extremes and Northern Hemisphere Annular Mode Index (NAMI, also referred as Arctic Oscillation Index, AOI) derived from three data sources (Hadley Centre, NCEP1 and NCAR). For the annual series of precipitation extremes, consecutive dry days (CDD) show a higher correlation coefficient than other indices, indicating that CDD is more sensitive than others. On a seasonal basis, correlation coefficients between precipitation indices and NAMI in wintertime are highlighted, instead of other seasons. So the precipitation extremes in this study area are greatly related to Arctic Oscillation during the last cold season. In addition, correlation coefficients derived from NCAR data are generally larger than those from Hadley Centre and NCEP1.

Table 4
Correlation coefficients between precipitation indices derived from gridded data and annual/seasonal Northern Hemisphere Annular Mode Index (NAMI) from different data sources.

	Annual	Winter (DJF)	Spring (MAM)	Summer (JJA)	Autumn (SON)
NAMI derived from Hadley Centre					
Precipitation	0.09	0.31*	0.09	0.05	−0.02
RX5day	0.03	0.24	0.01	0.23	−0.08
SDII	0.09	0.32*	0.03	0.06	−0.09
CDD	−0.33*	−0.30*	−0.25	−0.27	−0.32*
R95p	0.08	0.35*	0.07	0.09	−0.07
NAMI derived from NCEP1					
Precipitation	0.05	0.28*	0.07	−0.01	−0.07
RX5day	−0.02	0.22	0.00	0.16	−0.15
SDII	0.07	0.30*	0.04	0.01	−0.15
CDD	−0.23	−0.28*	−0.16	−0.15	−0.22
R95p	0.05	0.34*	0.07	0.03	−0.13
NAMI derived from NCAR					
Precipitation	0.23	0.32*	0.20	0.37**	0.06
RX5day	0.16	0.28*	0.11	0.40**	−0.01
SDII	0.25	0.36*	0.15	0.36**	−0.01
CDD	−0.29*	−0.23	−0.24	−0.32*	−0.24
R95p	0.24	0.38**	0.19	0.41**	0.02

*Statistically significant at the level of 0.05. ** Statistically significant at the level of 0.01.

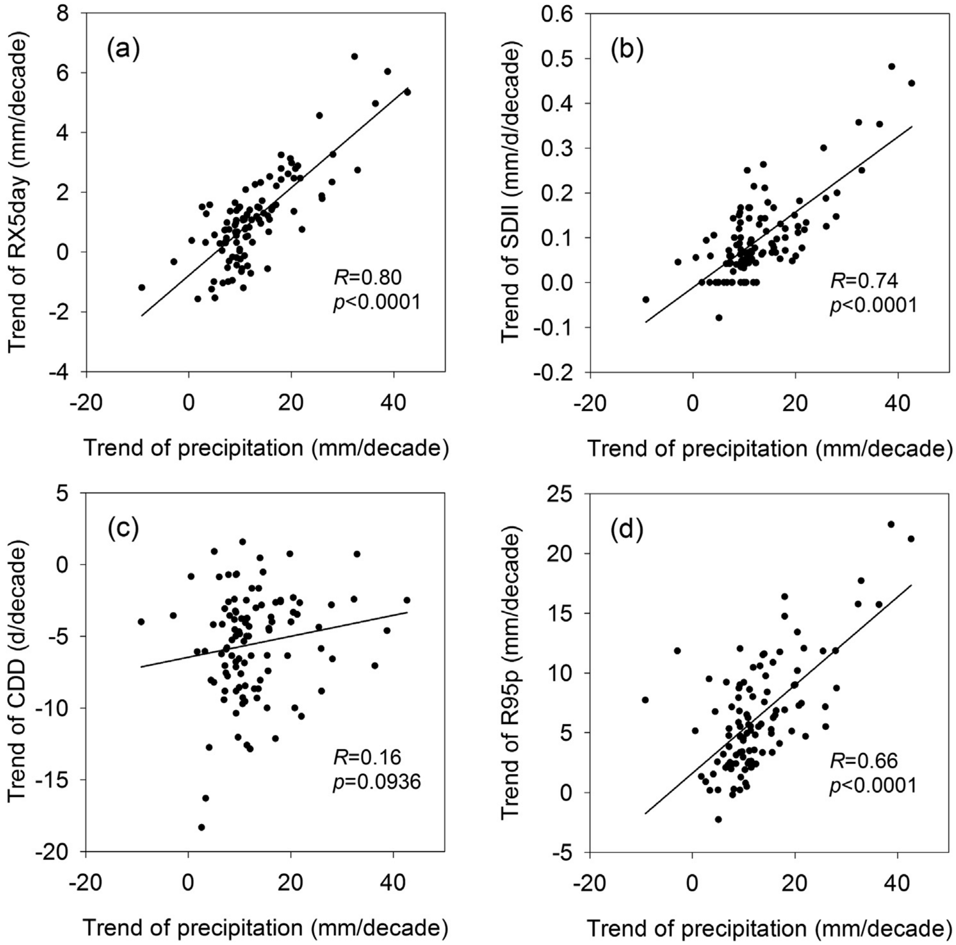

Fig. 8. Correlation between annual trend magnitudes between precipitation indices and total precipitation ($N = 105$). R is correlation coefficient, and p is significant level of t-test.

Fig. 10 shows the distribution of correlation coefficients between precipitation indices and NAMI. Correlation coefficients for most grid boxes show a spatial coherence, which is consistent with the regional trend of precipitation indices. The proportion of positive coefficient is 82.9%, 90.5% and 96.2% for maximum 5-day precipitation (RX5day), simple daily intensity index (SDII) and very wet day precipitation (R95p), respectively, while that of negative coefficient is 78.1% for consecutive dry days (CDD). The proportion with absolute value of coefficient larger than 0.2 is 20.0%, 39.0%, 42.9% and 40.0% for RX5day, SDII, CDD and R95p, while that larger than 0.1 is 77.1%, 70.5%, 65.7% and 83.8%. Correlation coefficients at eight observed stations are also added in Fig. 10. The observed values generally present similar patterns as the gridded ones.

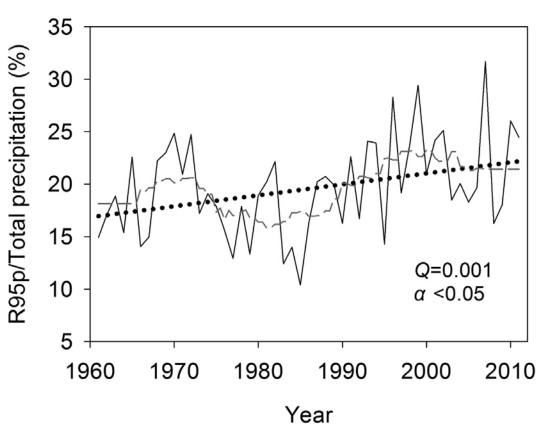

Fig. 9. Regional series for the ratio between very wet day precipitation (R95p) and annual total precipitation derived form gridded data. Q is Sen's slope in value per year, and α is significant level of Mann–Kendall test.

4. Discussion and conclusions

According to the daily precipitation data in alpine areas of the Chinese Tianshan Mountains, extreme precipitation events have significantly changed during the period 1961–2011. Due to the mountainous terrain, the long-term meteorological observation is relatively limited in the Chinese Tianshan Mountains. Compared with previous reports (Klein Tank et al., 2006), this study provides more detailed information about the climate extremes in arid central Asia, especially for the remote areas. Long-term changes in the selected precipitation indices exhibit a great wetting trend with spatial coherence over the Chinese Tianshan Mountains. Maximum 5-day precipitation, simple daily intensity index and very wet day precipitation show a significantly increasing trend, while consecutive dry days have decreased during the past five decades.

Compared with previous studies (Wang B. et al., 2013; Wang H. et al., 2013a,b; Jiang et al., 2012) covering larger areas with more non-alpine stations in Northwest China, the Chinese Tianshan Mountains suffer more significant changes in precipitation extremes. For example, the trend in consecutive dry days is −5.83 days per decade in the Chinese Tianshan Mountains during the

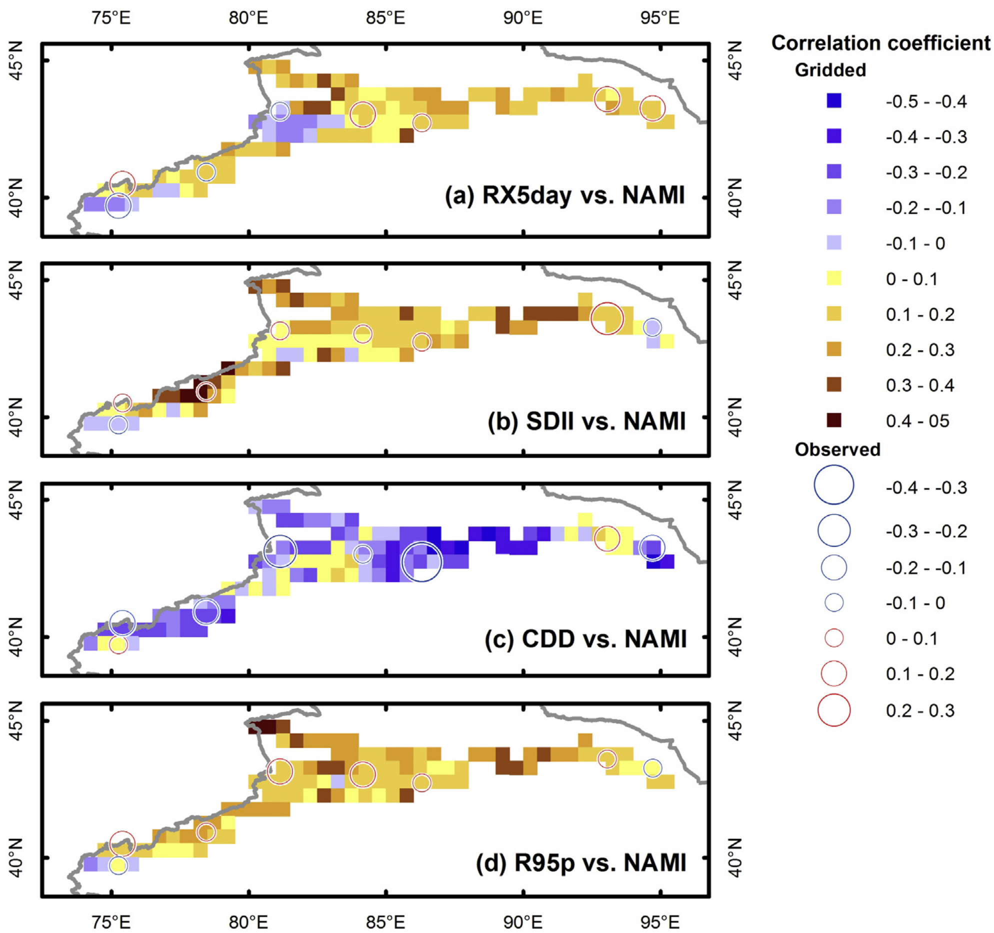

Fig. 10. Correlation coefficient between precipitation indices and wintertime Northern Hemisphere Annular Mode Index (NAMI) derived from Hadley Centre data.

period 1961–2011. However, the trend magnitude is just −1.72 days per decade in Xinjiang (21.2% of stations with altitude higher than 1500 m) from 1959 to 2008 (Jiang et al., 2012). For a greater area of Northwest China where Xinjiang belongs to, the trend magnitude is −2.52 (period 1960–2003) and −4.85 (period 1960–2010) days per decade respectively in different researches (Wang H. et al., 2013a,b). Another instance of maximum 5-day precipitation also shows differences, and the trends in the Chinese Tianshan Mountains, Xinjiang and Northwest China are 1.18 (period 1961–2011), 0.85 (period 1960–2009) and 0.98 (period 1960–2010) mm per decade, respectively, which is statistically significant at the 0.05 level (Wang B. et al., 2013; Wang H. et al., 2013a). It is clear that the changes in precipitation extremes in alpine areas are more significant than those in low-lying plains.

The increase of precipitation may cause a series of ecological, environmental and social sequences (Piao et al., 2010). The Tianshan Mountains are the sources of a number of interior rivers in central Asia, and most of the population lives in oasis belts at the low-lying plains and basins. Heavy precipitation events may provide more water to the mountainous areas, and then supply river runoff and ground water which are vital for the arid lower reaches (Xu et al., 2008; Zhao et al., 2010b). However, rainfall enhancement also raises the risk of flash flood and secondary disaster for human beings. In addition, with climate warming, the cryosphere in the Chinese Tianshan Mountains is experiencing a great melting in the past decades (Liu et al., 2006; Wang et al., 2011). The enhancement of atmospheric precipitation may theoretically slow down the glacier retreat, but the influence is too weak to effectively counteract the effect of air temperature rise (Li et al., 2011; Zhang et al., 2012a).

The potential linkage between precipitation extremes and large-scale atmospheric circulation is widely reported (Busuioc et al., 2001; Wang and Zhou, 2005; Houssos et al., 2008; Toreti et al., 2010; You et al., 2011). The trend magnitudes of precipitation extremes are greatly related to the enhanced total precipitation over the Chinese Tianshan Mountains. The regional vapor sources are mainly from the Atlantic Ocean and Arctic Ocean via the Westerlies. The Northern Hemisphere Annular Mode Index, (also referred as Arctic Oscillation Index) reflects the Westerlies in middle latitude of Northern Hemisphere. Previous researches have detected the relationship between Arctic Oscillation (North Atlantic Oscillation) and precipitation variation (Scaife et al., 2008; Yadav et al., 2009; Hu and Feng, 2010; Mao et al., 2011). Statistically significant correlations between precipitation indices and Northern Hemisphere Annular Mode Index occur in wintertime, which indicates the precipitation extremes in this study area are related to the Arctic Oscillation. However, the influence of circulation system is complex, and more detailed analyses are needed for further understanding of the internal regimes.

Urbanization and other human process can affect the observed meteorological records, including precipitation and evaporation (Allan, 2011; Min et al., 2011). Differing from a densely-populated metropolis, the anthropogenic effect may be generally slight for the remote mountains. According to the population standard of urban stations (50,000 or more) mentioned by Easterling et al. (1997), the observed eight stations in this study are classified as urban or rural stations, respectively. As recorded in the 5th national population census of China in 2000, the population for each town where these stations are located is less than 50,000, and at some remote stations is only about 4000 (Baluntai town). So, the local human-induced changes are not the main factor influencing climate extremes in this study.

Acknowledgments

This study was supported by the National Basic Research Program of China (973 Program) (No. 2013CBA01801), the National Natural Science Foundation of China (No. 41161012, 41240001), the Basic Scientific Research Foundation in University of Gansu Province, and the Fostering Foundation for the Excellent Ph.D. Dissertation of Northwest Normal University. We are very grateful to Zhaodong Feng and an anonymous reviewer for their constructive suggestions. Thanks also to the editorial staff.

References

Aizen, V.B., Aizen, E.M., Melack, J.M., Dozier, J., 1997. Climatic and hydrologic changes in the Tien Shan, Central Asia. Journal of Climate 10, 1393–1404.

Aizen, V.B., Kuzmichenok, V.A., Surazakov, A.B., Aizen, E.M., 2006. Glacier changes in the central and northern Tien Shan during the last 140 years based on surface and remote–sensing data. Annals of Glaciology 43, 202–213.

Allan, R.P., 2011. Climate change: human influence on rainfall. Nature 470, 344–345.

Bolch, T., 2007. Climate change and glacier retreat in northern Tien Shan (Kazakhstan/Kyrgyzstan) using remote sensing data. Global and Planetary Change 56, 1–12.

Busuioc, A., Chen, D., Hellström, C., 2001. Temporal and spatial variability of precipitation in Sweden and its link with the large–scale atmospheric circulation. Tellus A 53, 348–367.

Caesar, J., Alexander, L.V., Trewin, B., Tse-ring, K., Sorany, L., Vuniyayawa, V., Keosavang, N., Shimana, A., Htay, M.M., Karmacharya, J., Jayasinghearachchi, D.A., Sakkamart, J., Soares, E., Hung, L.T., Thuong, L.T., Hue, C.T., Dung, N.T.T., Hung, P.V., Cuong, H.D., Cuong, N.M., Sirabaha, S., 2011. Changes in temperature and precipitation extremes over the Indo–Pacific region from 1971 to 2005. International Journal of Climatology 31, 791–801.

Easterling, D.R., Horton, B., Jones, P.D., Peterson, T.C., Karl, T.R., Parker, D.E., Salinger, M.J., Razuvayev, V., Plummer, N., Jamason, P., Folland, C.K., 1997. Maximum and minimum temperature trends for the globe. Science 277, 364–367.

Getirana, A.C.V., Espinoza, J.C.V., Ronchail, J., Rotunno Filho, O.C., 2011. Assessment of different precipitation datasets and their impacts on the water balance of the Negro River basin. Journal of Hydrology 404, 304–322.

Gong, D.-Y., Ho, C.-H., 2003. Arctic oscillation signals in the East Asian summer monsoon. Journal of Geophysical Research 108, 4066. http://dx.doi.org/10.1029/2002JD002193.

Gu, W., Li, C., Li, W., Zhou, W., Chan, J.C.L., 2009. Interdecadal unstationary relationship between NAO and east China's summer precipitation patterns. Geophysical Research Letters 36, L13702. http://dx.doi.org/10.1029/2009GL038843.

Hoekstra, A.Y., Mekonnen, M.M., Chapagain, A.K., Mathews, R.E., Richter, B.D., 2012. Global monthly water scarcity: blue water footprints versus blue water availability. PLoS ONE 7, e32688. http://dx.doi.org/10.1371/journal.pone.0032688.

Houssos, E.E., Lolis, C.J., Bartzokas, A., 2008. Atmospheric circulation patterns associated with extreme precipitation amounts in Greece. Advances in Geosciences 17, 5–11.

Hu, Q., Feng, S., 2010. Influence of the Arctic oscillation on central United States summer rainfall. Journal of Geophysical Research 115, D01102. http://dx.doi.org/10.1029/2009JD011805.

Jiang, F., Hu, R.-J., Wang, S.-P., Zhang, Y.-W., Tong, L., 2012. Trends of precipitation extremes during 1960–2008 in Xinjiang, the Northwest China. Theoretical and Applied Climatology. http://dx.doi.org/10.1007/s00704-012-0657-3.

Ju, J., Lv, J., Cao, J., Ren, J., 2005. Possible impacts of the Arctic Oscillation on the interdecadal variation of summer monsoon rainfall in East Asia. Advances in Atmospheric Sciences 22, 39–48.

Kendall, M.R., 1955. Rank Correlation Methods. Charles Griffin, London, pp. 1–196.

Kezer, K., Matsuyama, H., 2006. Decrease of river runoff in the Lake Balkhash basin in Central Asia. Hydrological Processes 20, 1407–1423.

Klein Tank, A.M.G., Peterson, T.C., Quadir, D.A., Dorji, S., Zou, X., Tang, H., Santhosh, K., Joshi, U.R., Jaswal, A.K., Kolli, R.K., Sikder, A.B., Deshpande, N.R., Revadekar, J.V., Yeleuova, K., Vandasheva, S., Faleyeva, M., Gomboluudev, P., Budhathoki, K.P., Hussain, A., Afzaal, M., Chandrapala, L., Anvar, H., Amanmurad, D., Asanova, V.S., Jones, P.D., New, M.G., Spektorman, T., 2006. Changes in daily temperature and precipitation extremes in central and south Asia. Journal of Geophysical Research 111, D16105. http://dx.doi.org/10.1029/2005JD006316.

Li, J., Xiong, A., 2004. Summary of research on meteorological scientific data sharing system. Journal of Applied Meteorological Science 15, 1–9 (in Chinese).

Li, J.P., Wang, J.X.L., 2003. A modified zonal index and its physical sense. Geophysical Research Letters 30, 1632. http://dx.doi.org/10.1029/2003GL017441.

Li, Z., He, Y., Wang, P., Theakstone, W.H., An, W., Wang, X., Lu, A., Zhang, W., Cao, W., 2012. Changes of daily climate extremes in southwestern China during 1961–2008. Global and Planetary Change 80–81, 255–272.

Li, Z., Jiang, F., 2007. A study of abrupt climate change in Xinjiang Region during 1961–2004. Journal of Glaciology and Geocryology 29, 351–359 (in Chinese).

Li, Z., Li, H., Chen, Y., 2011. Mechanisms and simulation of accelerated shrinkage of continental glaciers: a case study of Urumqi Glacier No. 1 in eastern Tianshan, Central Asia. Journal of Earth Science 22, 423–430.

Li, Z., Wang, W., Zhang, M., Wang, F., Li, H., 2010. Observed changes in streamflow at the headwaters of the Urumqi River, eastern Tianshan, central Asia. Hydrological Processes 24, 217–224.

Lioubimtseva, E., Cole, R., Adams, J.M., Kapustin, G., 2005. Impacts of climate and land–cover changes in arid lands of Central Asia. Journal of Arid Environments 62, 285–308.

Lioubimtseva, E., Henebry, G.M., 2009. Climate and environmental change in arid Central Asia: impacts, vulnerability, and adaptations. Journal of Arid Environments 73, 963–977.

Liu, S., Ding, Y., Shangguan, D., Zhang, Y., Li, J., Han, H., Wang, J., Xie, C., 2006. Glacier retreat as a result of climate warming and increased precipitation in the Tarim river basin, northwest China. Annals of Glaciology 43, 91–96.

Mao, R., Gong, D.-Y., Yang, J., Bao, J.-D., 2011. Linkage between the Arctic oscillation and winter extreme precipitation over central–southern China. Climate Research 50, 187–201.

Marchenko, S.S., Gorbunov, A.P., Romanovsky, V.E., 2007. Regional changes of permafrost in Central Asia. Global and Planetary Change 56, 311–327.

Min, S.-K., Zhang, X., Zwiers, F.W., Hegerl, G.C., 2011. Human contribution to more–intense precipitation extremes. Nature 470, 378–381.

Narama, C., Kääb, A., Duishonakunov, M., Abdrakhmatov, K., 2010. Spatial variability of recent glacier area changes in the Tien Shan Mountains, Central Asia, using Corona (∼1970), Landsat (∼2000), and ALOS (∼2007) satellite data. Global and Planetary Change 71, 42–54.

NMIC (National Meteorological Information Center), 2012. Assessment Report of China's Ground Precipitation $0.5^{\circ} \times 0.5^{\circ}$ Gridded Dataset (V2.0). NMIC, Beijing.

Ogi, M., Tachibana, Y., Yamazaki, K., 2003. Impact of the wintertime North Atlantic Oscillation (NAO) on the summertime atmospheric circulation. Geophysical Research Letters 30, 1704. http://dx.doi.org/10.1029/2003GL017280.

Oki, T., Kanae, S., 2006. Global hydrological cycles and world water resources. Science 313, 1068–1072.

Piao, S., Ciais, P., Huang, Y., Shen, Z., Peng, S., Li, J., Zhou, L., Liu, H., Ma, Y., Ding, Y., Friedlingstein, P., Liu, C., Tan, K., Yu, Y., Zhang, T., Fang, J., 2010. The impacts of climate change on water resources and agriculture in China. Nature 467, 43–51.

Scaife, A.A., Folland, C.K., Alexander, L.V., Moberg, A., Knight, J.R., 2008. European climate extremes and the North Atlantic Oscillation. Journal of Climate 21, 72–83.

Schiemann, R., Lüthi, D., Vidale, P.L., Schär, C., 2008. The precipitation climate of Central Asia – intercomparison of observational and numerical data sources in a remote semiarid region. International Journal of Climatology 28, 295–314.

Sen, P.K., 1968. Estimates of the regression coefficient based on Kendall's tau. Journal of the American Statistical Association 63, 1379–1389.

Shi, Y., Shen, Y., Kang, E., Li, D., Ding, Y., Zhang, G., Hu, R., 2007. Recent and future climate change in northwest China. Climatic Change 80, 379–393.

Small, E.E., Giorgi, F., Sloan, L.C., 1999. Regional climate model simulation of precipitation in central Asia: mean and interannual variability. Journal of Geophysical Research 104, 6563–6582.

Sneyers, R., 1990. On the Statistical Analysis of Series of Observations. Technical Note 143. World Meteorological Organization, Geneva, Switzerland.

Thompson, D.W.J., Wallace, J.M., 2000. Annular modes in the extratropical circulation. Part I: month–to–month variability. Journal of Climate 13, 1000–1016.

Toreti, A., Xoplaki, E., Maraun, D., Kuglitsch, F.G., Wanner, H., Luterbacher, J., 2010. Characterisation of extreme winter precipitation in Mediterranean coastal sites and associated anomalous atmospheric circulation patterns. Natural Hazards and Earth System Science 10, 1037–1050.

Vincent, L.A., Aguilar, E., Saindou, M., Hassane, A.F., Jumaux, G., Roy, D., Booneeady, P., Virasami, R., Randriamarolaza, L.Y.A., Faniriantsoa, F.R., Amelie, V., Seeward, H., Montfraix, B., 2011. Observed trends in indices of daily and extreme temperature and precipitation for the countries of the western Indian Ocean, 1961–2008. Journal of Geophysical Research 116, D10108. http://dx.doi.org/10.1029/2010JD015303.

Vörösmarty, C.J., Green, P., Salisbury, J., Lammers, R.B., 2000. Global water resources: vulnerability from climate change and population growth. Science 289, 284–288.

Wang, B., 2004. A study on synthetic differentiation method for basic meteorological data quality control. Journal of Applied Meteorological Science 15, 51–59 (in Chinese).

Wang, B., Zhang, M., Wei, J., Wang, S., Li, S., Ma, Q., Li, X., Pan, S., 2013. Changes in extreme events of temperature and precipitation over Xinjiang, northwest China, during 1960–2009. Quaternary International 298, 141–151.

Wang, H., Chen, Y., Chen, Z., 2013a. Spatial distribution and temporal trends of mean precipitation and extremes in the arid region, northwest of China, during 1960–2010. Hydrological Processes 27, 1807–1818.

Wang, H., Chen, Y., Xun, S., Lai, D., Fan, Y., Li, Z., 2013b. Changes in daily climate extremes in the arid area of northwestern China. Theoretical and Applied Climatology 112, 15–28.

Wang, S., Zhang, M., Wang, B., Sun, M., Li, X., 2013. Recent changes in daily extremes of temperature and precipitation over the western Tibetan Plateau, 1973–2011. Quaternary International. http://dx.doi.org/10.1016/j.quaint.2013.03.037.

Wang, S., Zhang, M., Li, Z., Wang, F., Li, H., Li, Y., Huang, X., 2011. Glacier area variation and climate change in the Chinese Tianshan Mountains since 1960. Journal of Geographical Sciences 21, 263–273.

Wang, X.L., 2008. Accounting for autocorrelation in detecting mean shifts in climate data series using the penalized maximal *t* or *F* test. Journal of Applied Meteorology and Climatology 47, 2423–2444.

Wang, Y., Zhou, L., 2005. Observed trends in extreme precipitation events in China during 1961–2001 and the associated changes in large–scale circulation. Geophysical Research Letters 32, L09707. http://dx.doi.org/10.1029/2005GL022574.

Wang, Y., Wang, J., Qi, Y., Yan, C., 2005. Dataset of Desert Distribution in China (1: 100,000). Environmental and Ecological Science Data Center for West China, National Natural Science Foundation of China, Lanzhou, China. http://dx.doi.org/10.3972/westdc.006.2013.db.

Xu, J., Chen, Y., Ji, M., Lu, F., 2008. Climate change and its effects on runoff of Kaidu River, Xinjiang, China: a multiple time–scale analysis. Chinese Geographical Science 18, 331–339.

Yadav, R.K., Rupa Kumar, K., Rajeevan, M., 2009. Increasing influence of ENSO and decreasing influence of AO/NAO in the recent decades over northwest India winter precipitation. Journal of Geophysical Research 114, D12112. http://dx.doi.org/10.1029/2008JD011318.

You, Q., Kang, S., Aguilar, E., Pepin, N., Flügel, W.-A., Yan, Y., Xu, Y., Zhang, Y., Huang, J., 2011. Changes in daily climate extremes in China and its connection to the large scale atmospheric circulation during 1961–2003. Climate Dynamics 36, 2399–2417.

You, Q., Kang, S., Pepin, N., Yan, Y., 2008. Relationship between trends in temperature extremes and elevation in the eastern and central Tibetan Plateau, 1961–2005. Geophysical Research Letters 35, L04704. http://dx.doi.org/10.1029/2007GL032669.

Zhang, X., Yang, F., 2004. RClimDex (1.0) User Manual. Climate Research Branch, Environment Canada, Ontario, Canada.

Zhang, X., Zhang, J., 2006. Handbook of Xinjiang Meteorology. China Meteorological Press, Beijing, pp. 132–156 (in Chinese).

Zhao, L., Wu, Q., Marchenko, S.S., Sharkhuu, N., 2010a. Thermal state of permafrost and active layer in Central Asia during the international polar year. Permafrost and Periglacial Processes 21, 198–207.

Zhao, W.Y., Chen, Y.N., Li, J.L., Jia, G.S., 2010b. Periodicity of plant yield and its response to precipitation in the steppe desert of the Tianshan Mountains region. Journal of Arid Environments 74, 445–449.

Zhang, M., Wang, S., Li, Z., Wang, F., 2012a. Glacier area shrinkage in China and its climatic background during the past half century. Journal of Geographical Sciences 22, 15–28.

Zhang, Q., Singh, V.P., Li, J., Jiang, F., Bai, Y., 2012b. Spatio–temporal variations of precipitation extremes in Xinjiang, China. Journal of Hydrology 434–435, 7–18.